

Perspective

Disease Diagnosis with Chemosensing, Artificial Intelligence, and Prospective Contributions of Nanoarchitectonics

Xuechen Shen^{1,2,*} and Katsuhiko Ariga^{1,2,*} ¹ Graduate School of Frontier Sciences, The University of Tokyo, 5-1-5 Kashiwanoha, Kashiwa 277-8561, Japan² Research Center for Materials Nanoarchitectonics (MANA), National Institute for Materials Science (NIMS), 1-1 Namiki, Tsukuba 305-0044, Japan

* Correspondence: 2631202228@edu.k.u-tokyo.ac.jp (X.S.); ariga.katsuhiko@nims.go.jp (K.A.)

Abstract: In modern materials research, nanotechnology will play a game-changing role, with nanoarchitectonics as an overarching integrator of the field and artificial intelligence hastening its progress as a super-accelerator. We would like to discuss how this schema can be utilized in the context of specific applications, with exemplification using disease diagnosis. In this paper, we focus on early, noninvasive disease diagnosis as a target application. In particular, recent trends in chemosensing in the detection of cancer and Parkinson's disease are reviewed. The concept has been gaining traction as dynamic volatile metabolite profiles have been increasingly associated with disease onset, making them promising diagnostic tools in early stages of disease. We also discuss advances in nanoarchitectonic chemosensors, which are theoretically ideal form factors for diagnostic chemosensing devices. Last but not least, we shine the spotlight on the rise to prominence and emergent contributions of artificial intelligence (AI) in recent works, which have elucidated a strong synergy between chemosensing and AI. The powerful combination of nanoarchitectonic chemosensors and AI could challenge our current notions of disease diagnosis. Disease diagnosis and detection of emerging viruses are important challenges facing society. The parallel development of advanced functional materials for sensing is necessary to support and enable AI methodologies in making technological leaps in applications. The material and structural formative technologies of nanoarchitectonics are critical in meeting these challenges.



Citation: Shen, X.; Ariga, K. Disease Diagnosis with Chemosensing, Artificial Intelligence, and Prospective Contributions of Nanoarchitectonics. *Chemosensors* **2023**, *11*, 528. <https://doi.org/10.3390/chemosensors11100528>

Academic Editors: Priscila Aléssio and Maria Braunger

Received: 6 July 2023

Revised: 16 September 2023

Accepted: 27 September 2023

Published: 7 October 2023



Copyright: © 2023 by the authors. Licensee MDPI, Basel, Switzerland. This article is an open access article distributed under the terms and conditions of the Creative Commons Attribution (CC BY) license (<https://creativecommons.org/licenses/by/4.0/>).

Keywords: artificial intelligence; noninvasive disease diagnosis; chemosensing; cancer; Parkinson's disease; nanoarchitectonics

1. Introduction

Advances in materials science such as the development of nanotechnology provide the means to solve a variety of problems in energy [1–15], the environment [16–31], and medicine [32–48]. More specifically, advances in nanotechnology have made it possible to observe small structures, analyze their properties, and manipulate structures at fundamental levels [49–59]. Using materials science principles, functional materials with higher performance and specificity are now being developed through the creation of groups of materials with ever more precise internal nanostructures. The overarching concept that encompasses systematizing the body of knowledge about these materials and facilitating new developments is nanoarchitectonics [60,61]. Nanoarchitectonics emerged as a post-nanotechnological concept [62]. Richard Feynman founded the concept of nanotechnology in the mid-20th century [63,64], and Masakazu Aono proposed nanoarchitectonics at the beginning of the 21st century [65,66]. Nanoarchitectonics integrates nanotechnology with other fields of materials science. It is the architecting of functional material groups from atoms, molecules, and nanomaterials [67–69]. Since all materials are made of atoms and molecules, this methodology theoretically applies in the creation of all materials. It may be likened to the theory of everything in physics [70] and may be considered the method for everything in materials science [71].

When developing new materials for a purpose, it is crucial to sift through the breadth of established knowledge for a method that is suitable and effective. Until now, scientists have achieved this through experience, intuition, and honed literature searches. In recent years, however, artificial intelligence (AI) technologies have advanced remarkably; machine learning (ML) [72–79] and materials informatics [80–87] now demonstrate considerable potential to support the work of scientists, on the premise of large amounts of accumulated data. This may give nanoarchitectonics, which aims to integrate many kinds of materials and diverse properties, a significant edge against the evolving challenges and demands of today. In modern materials research, nanotechnology will play a game-changing role, with nanoarchitectonics as an overarching integrator of the field, and AI hastening its progress as a super-accelerator [88]. The effectiveness of such a schema has been anticipated in the field of nanoporous materials used for energy applications. The same strategy could bring efficiency and productivity to a variety of fields and targets under nanoarchitectonics. It is known to be useful in the field of biotechnology, encompassing basic biological [89–92] and biomedical applications [93–96]. It also has notable applications in various chemical sensors [97–101] and biosensors [102–106]. There is a high possibility for nanoarchitectonics to make major contributions to sensing in biological systems, which is necessary to address modern healthcare demands.

With this background, we would like to discuss how the schema can be utilized in specific applications. In this paper, we focus on early, noninvasive disease diagnosis as a target application. In particular, there have been recent, exciting developments in chemosensing in the detection of cancer and Parkinson's disease, which are the focusing lens of this review. Our review explores the growing prominence and contributions of AI to chemosensing diagnostics. Through examples in recent literature, we frame a portrait of the complementary nature of nanoarchitectonic chemosensors and AI, and how they are congregating to challenge our current notions of disease diagnosis. Finally, we close by conveying our perspectives on the abundant challenges and opportunities from a materials science standpoint.

2. Application of Chemosensing in Early, Noninvasive Disease Detection

Early, accurate diagnosis plays a key role in patient outcomes for any disease. In turn, extraction of biochemical data from biofluids is key to making early and accurate diagnoses. Both established diagnostic tools and ongoing research heavily favor analyzing invasively collected samples such as blood and tissue over noninvasive samples such as urine, breath, saliva, etc. Bujak et al. found that, in metabolomics research conducted between 2010 and 2015, 68.5% of studies were conducted on blood, 4.4% on tissue extracts, 21.3% on urine, and only 4.6% and 1.4% on saliva and breath samples, respectively [107]. The disadvantages of invasive sample collection are well known, including pain and discomfort for the patient, the necessity for assisted collection, and higher sampling, analysis, and storage costs. In comparison, breath, saliva, and other noninvasively collected biofluids are heavily under-utilized in both diagnosis and research.

Nonetheless, the heavy favor towards invasive sampling is not without reason. Noninvasive samples typically suffer from high levels of bacterial contamination and low analyte quality. However, newly discovered links between disease and volatile organic compounds (VOCs) emanating from noninvasive biofluids, new chemosensing approaches to analyzing those biofluids, and the integration of AI to interpret the data together warrant renewed interest in studying noninvasively collected biofluids as diagnostic tools.

There is a relatively mature and reliable methodology for studying and analyzing VOCs from biofluids (Figure 1). Following sample collection, gas-phase (e.g., breath) samples can be directly analyzed, while liquid-phase (e.g., urine) and solid-phase (e.g., tissue extracts) samples often undergo headspace analysis to enhance volatile components. VOCs derived from the sample typically undergo a combined technique of separation (e.g., by affinity, mass, ionization, electrophoresis, etc.) and spectrometry/spectroscopy (e.g., ion mobility, mass, NMR, etc.). The most common combination techniques are variations

of gas and liquid chromatography and mass spectrometry (GC-MS and LC-MS). More details on analytical techniques and their application to breath and saliva samples have been comprehensively reviewed elsewhere [108].

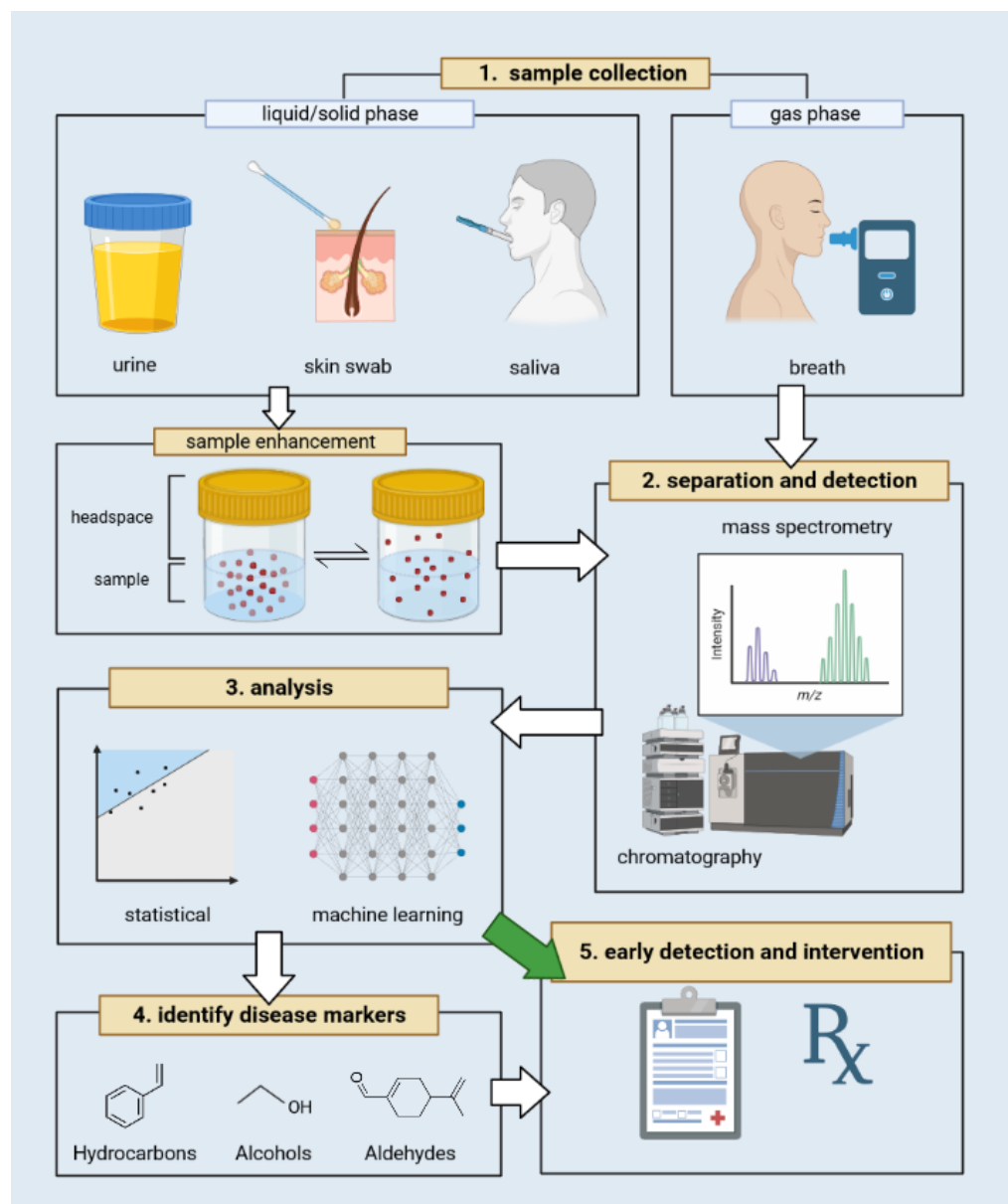


Figure 1. Schema for detecting disease with volatile organic compounds found in noninvasively collected biofluid samples: 1. The sample is noninvasively collected (liquid- and solid-phase samples may undergo headspace analysis to enhance volatile components); 2. Different molecular species are separated and identified (typically with a combination of chromatography and mass spectrometry); 3. The generated dataset is analyzed with statistical, and more recently, machine learning tools; 4. Biomarkers of disease are identified and validated; 5. Tests for biomarkers are developed to enable early disease detection and intervention.

Here, we review the newest developments in early, noninvasive detection of cancer and Parkinson's disease by covering two subsidiary topics—recent advancements in the established methodology using GC-MS and adjacent technologies (Section 2), and chemosensor developments under the nanoarchitectonics strategy with prospective contributions to the field (Section 3)—while portraying AI's rise to prominence in this field.

2.1. Chemosensing in Detecting Cancer

The altered metabolism of cancer cells leads to abnormalities in their biochemical pathways (i.e., changes in rate of oxidative stress, lipid peroxidation, and gene sequences). Consequently, the downstream products, including VOC profiles, are putatively distinguishable by more advanced olfactory systems. In the past decade, attempts have been made to harness fruit fly [109,110], canine [111,112], and murine [113] olfactory systems for cancer detection. In the absence of comparable artificial gas sensors, biological sensors have demonstrated the potential for chemosensing in the detection of cancer, but they also demonstrate inherent flaws such as ethical controversy, investment into training and sustaining animals, errors in interpreting animal behavior, lacking robustness and quantifiability, and being unsuitable for storage.

Recent studies have converged in their approaches towards early, noninvasive cancer screening. The aim is to identify key VOC biomarkers in samples of respective cancer types (i.e., breath samples for lung cancer (LC), urine samples for bladder cancer (BC)), so that gas sensing techniques and artificial gas sensors may be applied in cancer detection. Concomitantly, some studies further apply statistical and ML methods on identified VOCs and corresponding concentration dynamics to build predictive models that classify patient datasets into cancer-bearing and healthy groups.

Sani et al. used liquid chromatography–mass spectrometry (LC-MS) to detect and analyze VOCs in breath samples (291 LC patients and 95 healthy controls) [114]. They discovered seven VOCs with significantly different concentrations between LC patients and healthy controls, and built a predictive model based on a random forest algorithm. The dataset was evenly split into a training set and a validation set. The model achieved an average diagnostic sensitivity (rate of true positives) of 83% and specificity (rate of true negatives) of 78% based on those markers; the area under the curve (AUC) of the receiver operating characteristic (ROC) curve, plotting the rate of true positives (sensitivity) against the rate of false positives (1-specificity), ranged between 0.604 and 0.766 for the seven VOCs. They identified 3-hydroxy-2-butanone and 2-pentanone as candidate biomarkers of LC and associated their concentration dynamics with the sugar metabolism of oral bacteria and lipid metabolism in LC patients, respectively.

Wang et al. used high-pressure photon ionization–time-of-flight mass spectrometry (HIPPI-TOFMS) and identified 16 relevant VOC species in a discovery study of 84 LC patients [115]. Using a multivariate logistic regression model based on the 16 VOCs, they achieved a sensitivity of 89.2% and specificity of 89.1% in a validation study of 157 LC patients and 368 healthy controls, reaching an AUC of 0.952. Amongst the 16 VOCs, the authors surmised that the 8 most prominent VOCs in terms of diagnostic performance could be applied in lung cancer diagnosis. The same model trained on only the top eight VOCs yielded a sensitivity of 86% and specificity of 87.2%, reaching an AUC of 0.931.

Ligor et al. used headspace solid-phase microextraction (SPME) to extract VOCs from urine samples (40 BC patients and 57 healthy controls), and gas chromatography–time-of-flight-mass spectrometry (GC-TOF-MS) to detect and analyze gas components [116]. They discovered 12 VOCs exclusively present in the urine of BC patients, and 6 additional VOCs present in elevated levels. Among these identified species, they proposed butyrolactone, 2-methoxyphenol, 3-methoxy-5-methylphenol, 1-(2,6,6-trimethylcyclohexa-1,3-dien-1-yl)-2-buten-1-one, nootkatone, and 1-(2,6,6-trimethyl-1-cyclohexenyl)-2-buten-1-one as candidate biomarkers for detecting BC.

2.2. Chemosensing in Detecting Parkinson's Disease

Recent studies have led to significant milestones in detecting Parkinson's disease (PD) using sebum. Sebum is a biofluid secreted by sebaceous glands that aids the body with temperature regulation by moisturizing skin and trapping sweat. Increased sebum production has long been associated with seborrheic dermatitis (SD), which is a premotor symptom of PD caused by hormonal changes [117]. Some recent studies have shown a

significant correlation between PD and compositional changes in sebum, and the prospect of diagnosing PD with the aid of chemical sensing methods thereby.

Using LC-MS to separate and detect analytes, Sinclair et al. discovered differences in the metabolomic profiles of diagnosed PD patients compared with healthy controls; these include downregulation of ceramide, triacylglycerol, and fatty acyl classes and upregulation of glycosphingolipid and fatty acyl classes, which point to certain enriched metabolic pathways in PD patients [68]. Using paper spray ionization with ion mobility mass spectrometry (PS-IS-MS), Sarkar et al. aimed for faster analysis and reduced sample processing to improve clinical utility compared with LC-MS; this technique also allows the further separation of analytes by their mass-to-charge ratio [118]. They detected that higher-molecular-weight species such as triacylglycerides and diglycerides were expressed differently in PD patients [119].

In the chemosensing approach to PD screening, sebum samples are typically swabbed from skin in sebum-rich locations (upper back). Analytes are separated, analyzed, and cross-referenced with known biomarker profiles (Figure 2). The value proposition of the approach lies in establishing an objective and consistent diagnosis for PD, early detection preceding significant motor degeneration, and noninvasive, inexpensive sample collection [118–120].

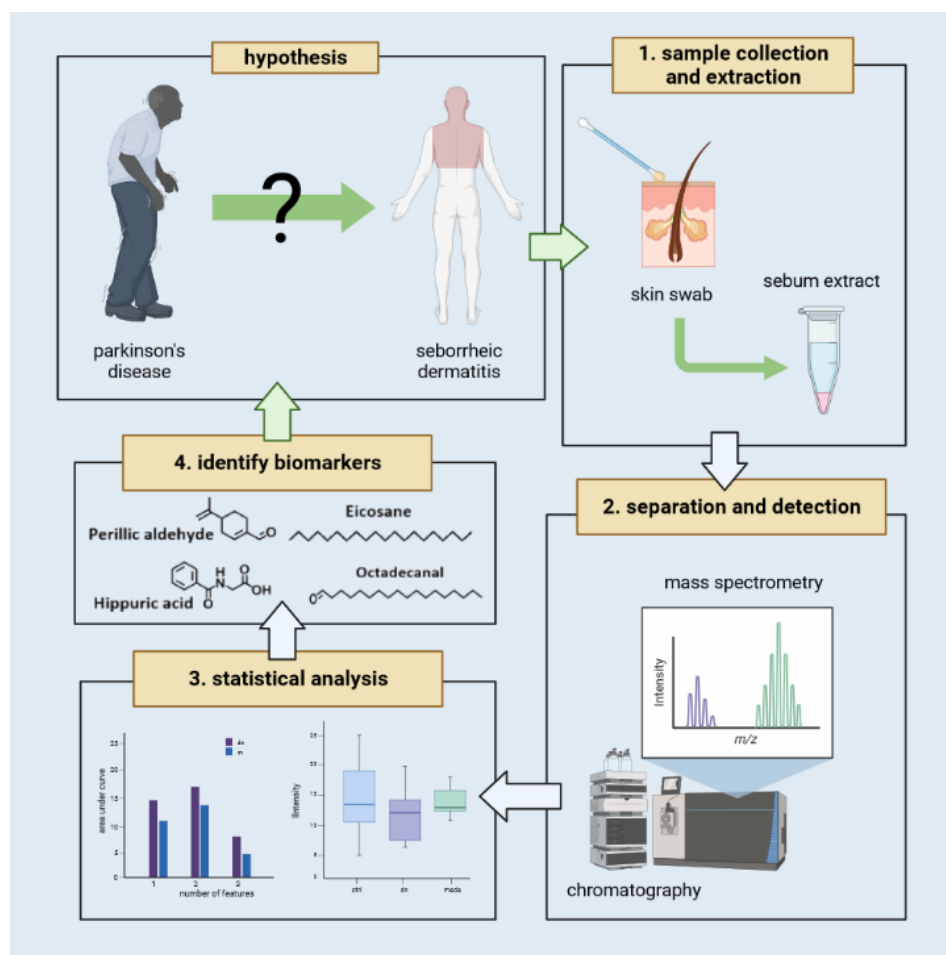


Figure 2. The idea of detecting Parkinson’s disease through odor derives from a “supersmeller” individual, and a hypothesis wherein seborrheic dermatitis is a premotor symptom of PD. The study of sebum as a biofluid from which PD biomarkers could be extracted was pioneered by Barran’s group [121], and several metabolomic and VOC biomarkers have been reported at the time of writing [118,119,122]. Besides having a key role in developing critical early diagnostic tools, the identified biomarkers may contribute to an improved understanding of the metabolic pathways that cause motor degeneration.

VOCs, as a class of metabolites, generated much of the initial interest in chemosensing for the detection of PD. These molecules contribute to a characteristic odor profile that was first reported by an individual with a remarkable sense of smell [121,123].

Using thermal desorption–gas chromatography–mass spectrometry (TD-GC-MS) for detection and analysis, Trivedi et al. identified a distinct volatile metabolomic profile associated with PD [121]. The pilot study (43 PD patients and 21 healthy controls) used a partial least-squares-discriminant analysis (PLS-DA) model to classify biomarker data, achieving a sensitivity of 90% and specificity of 67%, reaching an AUC of 0.777. They identified perillic aldehyde, eicosane, octadecanal, and hippuric acid as key biomarkers in PD patients; these findings were corroborated by the supersmeller individual.

In a follow-up study (100 PD patients and 29 healthy controls), Sinclair et al. added headspace analysis to concentrate samples before detection and again classified data to differentiate PD patients from controls using a PLS-DA model [122]. They achieved a sensitivity of 92.4% and specificity of 64.5%, which is consistent with the pilot study and reinforces the existence of a unique VOC profile associable with PD; ROC curve analysis yielded an AUC of 0.872, which is significantly improved from the pilot study, potentially due to larger sample size. However, retention times and spectra did not sufficiently match the four previously identified biomarkers, instead hinting at a more complex profile consisting of large, chemically similar hydrocarbon products of lipid decomposition.

2.3. Discussion and Evaluation of Chemosensing in Disease Detection

Although few would contend their existence at this point, the identity of viable VOC biomarkers of cancer is a subject of much contention. Various hydrocarbon, alcohol, and aldehyde groups have been detected with some frequency, but there has been no satisfying consensus on specific and targetable compounds [115]. This is unsurprising, as the inability to replicate results of metabolomics studies (and clinical studies in general) is widely acknowledged [108]. Small sample sizes, inconsistencies in sample collection, variation between individuals, patient condition, test environment, etc., are but some obstacles precluding confirmation of a working set of cancer biomarkers [108,115].

In the recent past, statistical techniques such as principal component analysis (PCA) and partial least squares (PLS) have been standard for building predictive models based on VOC biomarker data, with the aim of classifying diseased and healthy datasets for diagnostic purposes [108]. As is evident in the literature examples reviewed thus far, the recent trend is to build predictive models using ML techniques instead. ML techniques are certainly advantageous when dealing with multivariate and multidimensional problems like disease diagnosis, and the combined GC-MS/LC-MS techniques generate plenty of data for model training. Nevertheless, some ML techniques are prone to overfitting, particularly in studies with smaller sample sizes, and their black box nature further obfuscates the criteria for classification and dimension reduction. A comparative study evaluating the performance of some ML techniques applied to breast cancer detection was conducted by Wang [124].

At the time of writing, reported diagnostic accuracies (sample mean of sensitivity and specificity) of over 80% are common, and performances of 60–70% are considered poor [115]. Next to diagnostic accuracy, the most consistently reported indicator of a model's discriminatory power is the receiver operating characteristic (ROC), which is often summarized by its area under the curve (AUC). The ROC itself is a plot of the model's rate of true positives (sensitivity) against its rate of false positives (1–specificity). As such, the AUC is a value between 0 and 1.0, the higher the better, with values > 0.95 considered excellent, and values < 0.5 considered not useful in terms of screening performance [125–127]. Values between 0.5 and 0.95 are more difficult to interpret, and require closer scrutiny of the ROC's shape, standard deviation, mean, and sample size to draw conclusions [127]. As such, the interested reader is encouraged to refer to ROC plots from the primary sources to make a more extensive assessment of the studies' credibility.

Although the ROC is mathematically simple and overwhelmingly popular in the literature, the plot does not aptly facilitate comparison between different diagnostic tests. This has led to implicit comparison of AUC values in many studies, which has been implicated as meaningless because it fails to preserve contextual information upon derivation from the ROC, as detailed in Wald et al. [127].

Although other sophisticated supporting metrics such as likelihood ratios exist, they are currently seldom used and reported in the featured articles, and consequently do not facilitate comparison either. Indeed, the absence of a clearly defined, objective, and widely used or standardized metric and threshold is problematic for comparing the power of different diagnostic tests for screening purposes.

Furthermore, beyond being an objective metric, the clinical usefulness of a test is also strongly influenced by the prevalence of the disease to be diagnosed, implications and side effects of intervention, and cost and indications of a specific testing product. As such, in lieu of replacing professional diagnoses, the prospective role of this technology will likely be that of a powerful early monitoring and diagnostic tool, used alongside additional indicators, signs, and symptoms to help healthcare professionals make more objective and informed diagnoses.

Compared with the body of work on cancer biomarkers and diagnostics, studies on PD are fewer and less mature. The concept of extracting PD biomarkers from sebum was only pioneered in 2019. However, we can reasonably extrapolate much of the discourse on and trends in cancer biomarker and diagnostic studies to PD. As with cancer, detecting PD by direct verification of compounds currently presents considerable challenges due to the complexity of sebum composition. Although the mainstream studies presented thus far have exclusively developed statistical models, we can expect a future trend of exploring PD detection by recognizing features of the chemical profile using ML methods; in fact, one such study has already been published by Fu et al., and it features in Section 4 of this review [120].

A final issue with the established methodology for chemosensing in disease detection lies with its form factor. The GC-MS detectors and equivalent setups are bulky in size, and costly in time and resources to operate [120]. Furthermore, many studies are using increasingly specialized equipment that would not be widely accessible [115,116,119,121]. Due to these factors, the technique may not be particularly suitable for a clinical setting.

3. Developments in Nanoarchitectonics for Chemosensing in Disease Detection

Alongside the established GC-MS methodology, various chemosensors under the nanoarchitectonics design schema are being developed to capture and detect specific analytes. Although these sensors would not be as useful as the established GC-MS methodology for detecting a wide range of analytes, some demonstrate the potential to yield higher detection performances for their target analytes. These chemosensors would also exist in smaller form factors that are more suitable for clinical application.

Typically, these chemosensors operate by capturing gaseous analytes through adsorption, which is usually mediated by intermolecular interactions. As such, adsorption can be very selective towards target molecules. Once adsorbed, the sensor generates a cascading response imputably ending in perturbances in its electrical or spectral readout. The sensor may also demonstrate amplified responses to a target molecule, leading to extremely small detection limits. This combination of selectivity and sensitivity, and any synergy thereby derived, is why chemosensors are expected to demonstrate better detection performances than the more generalized GC-MS methodology towards a specific set of target analytes.

Sensing elements are typically nano- or microscale, with tens to hundreds of them implemented as gas sensor arrays. Advanced sensor arrays tend to have variations on the chemical or physical structure of sensing elements; this provides cross-referenceable signals that generate even more selectivity and sensitivity to target analytes. Such gas sensing arrays have featured prominently under the broad category of devices known as “electronic noses”.

Considering the numerous key advantages of chemosensors, they hold great promise as a product-to-market approach for disease detection. However, it must be noted that the above description paints an idealized portrayal of the theoretical advantages of chemosensors. In reality, existing methodologies allow for only crude control over adsorption and output characteristics. Tailoring a sensor design to a few specific target molecules remains as yet a laborious and futile exercise, making chemosensing a field that would benefit greatly from advancements in nanoarchitectonics methodologies. Nevertheless, good detection performances have been reported using a variety of generic and innovative sensor concepts, indicating increased interest in their use towards chemosensing in the detection of cancer.

Shang et al. developed a portable and wireless breath sensor array for screening LC (Figure 3) [128]. The sensor uses a nanoarchitectonics strategy with an array of differently patterned chemiresistive thin-film assemblies of gold nanoparticles to adsorb analytes, which causes changes in the film's dielectric properties and conductivity as it swells. Using the sensor, they demonstrated identification of common VOCs and LC-related VOCs with principal component analysis (PCA), demonstrating a limit of detection for some species as low as 6 ppb. The sensor could distinguish simulated breath samples, one representing healthy human breath, and others with varying concentrations of LC-related VOCs mixed in. Amongst the panel of LC-related VOCs, they identified 2-ethyl-4-methyl-1-pentanol as particularly well differentiated by the sensor from mundane VOCs in human breath.

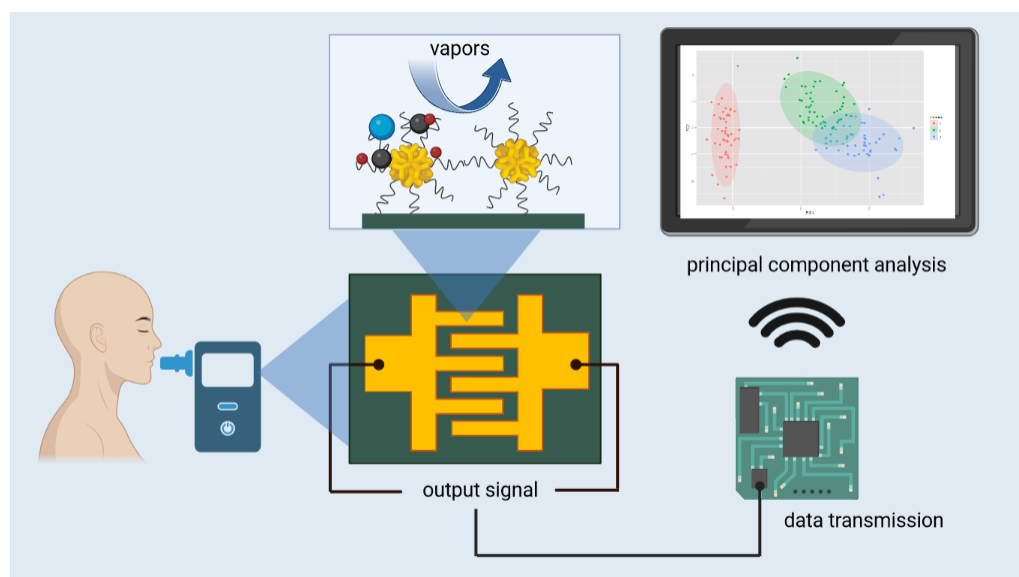


Figure 3. A chemiresistive gas sensor array that operates by adsorbing analyte gas molecules to gold nanoparticles; the nanoparticles are patterned in an interdigitated design, which generates an electrical signal and transmits it for data analysis. This sensor was developed by Shang et al. to detect lung cancer from breath samples [128].

Bhattacharyya et al. report a cost-effective and portable fluorometric sensor for BC-related VOCs in urine (Figure 4) [129]. The sensor consists of a sensor paper presenting Nile Red, Eosin Y, and Rose Bengal photosensitizer molecules. The cellulose sensor paper adsorbs VOCs from the headspace of urine samples, which interact with the photosensitizers to emit measurable UV-Vis absorption spectra. In particular, they found remarkable similarities between the spectra of crude ethyl benzene and BC patient urine samples, indicating significant generation of ethyl benzene related to BC pathology. Nevertheless, testing the sensor on actual urine samples yielded significantly higher (2–3 times) intensities, indicating that other VOCs also elicited responses from the photosensitizers. Using the sensor, they achieved a sensitivity of 87% and specificity of 86% on 52 BC patients and 33 healthy controls.

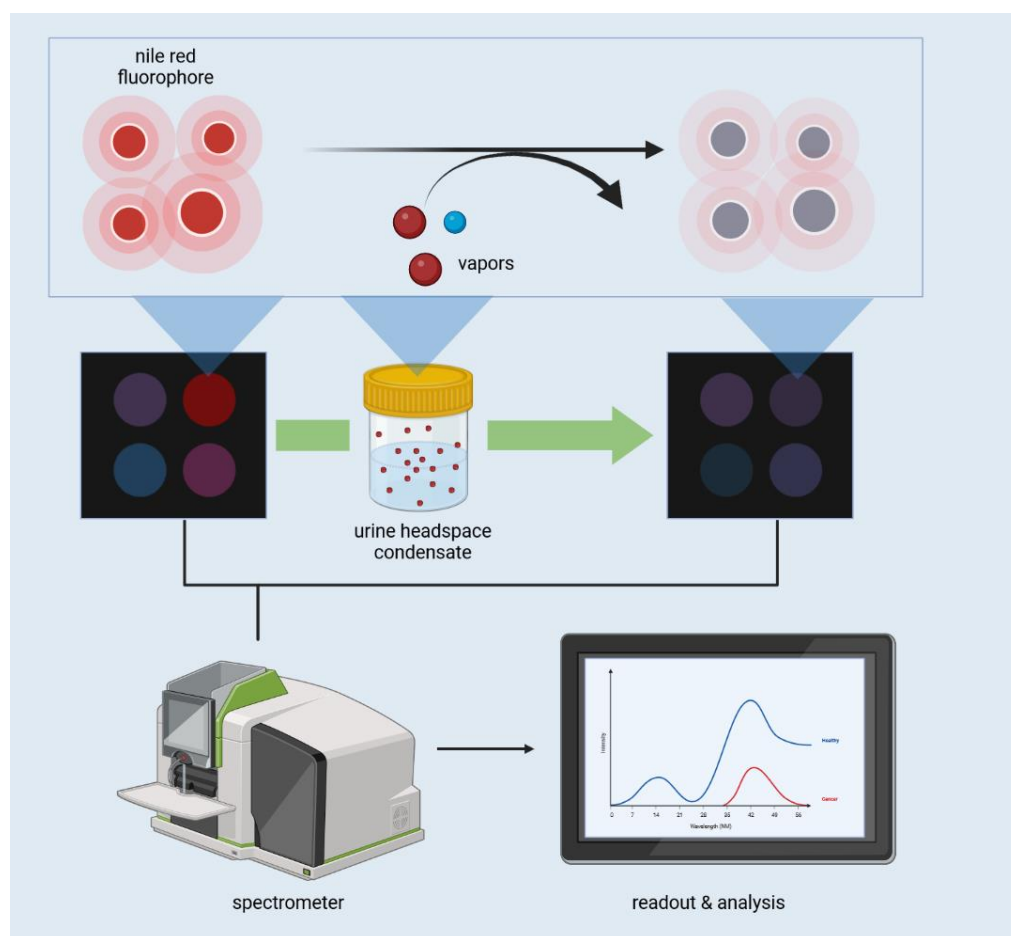


Figure 4. A fluorometric gas sensor array that operates by exposing analyte gas molecules to a sheet presenting different fluorophores; the analytes catalyze chemical transformations of the fluorophores and change their photonic properties to varying degrees. The change in fluorescence is read by an absorbance spectrometer and analyzed. This sensor was developed by Bhattacharyya et al. to detect bladder cancer from urine samples [129].

Jian et al. developed a chemiresistive sensor array for fast and noninvasive detection of BC from urine samples (Figure 5) [130]. The sensor consists of different doped PANI films with and without plasma treatments, designed for cross-reactive sensing of 11 BC-related VOCs. The films adsorb analytes to produce a change in its conductive properties; each film putatively recorded different responses to target VOCs, with the phosphoric acid-doped PANI film demonstrating high sensing performance against multiple target VOCs. A support vector machine (SVM) machine learning algorithm was implemented to recognize patterns in the sensor array signals and make diagnoses based on urine samples (76 BC patients and 18 healthy controls). The sensor achieved a remarkably high diagnostic accuracy of 96.67% (100% sensitivity and 83.33% specificity), with an AUC of 0.99. This study describes a sensor with promising diagnostic capabilities comparable to GC-MS, in a portable, fast, and cost-effective form factor. It demonstrates a powerful synergy between AI diagnostic tools and highly selective and specific sensors.

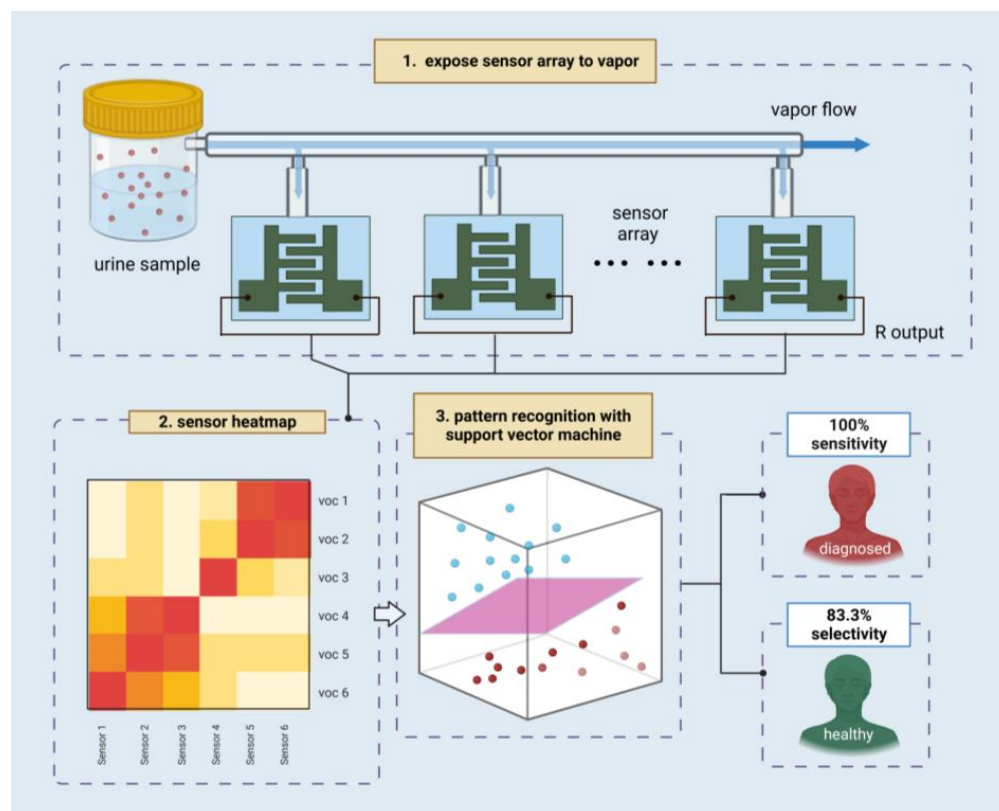


Figure 5. Jian et al. used a chemiresistive sensor array to detect bladder cancer from urine samples. An array of 10 differently doped PANI sensors produced correspondingly different responses to 11 target volatile organic compounds. The data were used to train a support vector machine algorithm, which performed highly accurate diagnoses of bladder cancer despite its small form factor [130].

4. Artificial Intelligence in Chemosensing Diagnostics

The prominent role of AI in recent works has been evident in our review. It has become pertinent to put AI in the spotlight, and discuss its accelerating impact on the field, comparison with past methods (statistical models), and prospective and as yet untapped potential for further impact.

A key advantage of harnessing animal olfactory systems or biological chemosensors is non-reliance on prior research to establish known chemical profiles or biomarkers. Typically, the chemical profile would also be too complex to break down into signatures of specific targetable molecules, as we have seen with cancer and PD. Tangentially, the discovery of a definitive set of biomarkers related to any disease is extremely rare. The recent boom in AI technologies may close the gap between biological and artificial chemosensors in this aspect.

Benet et al. performed a multidimensional breast cancer study, comparing the diagnostic efficacy of AI (convolutional neural network (CNN)) against statistical methods (PCA), and conventional GC-MS detection compared with their electronic nose prototype (Figure 6) [130]. Using GC-MS detection and PCA, they achieved an overall diagnostic accuracy of 77.11% (75.05% sensitivity and 68.33% specificity). The CNN model with four convolutional filters was trained on GC-MS data from 65 urine samples, tested on 12, and cross-validated with 13. Using GC-MS and CNN, they achieved a remarkably higher diagnostic accuracy of 92.31% (100% sensitivity and 95.71% specificity). Using the electronic nose prototype resulted in significantly lower diagnostic accuracies of 58.3% with PCA (75% sensitivity and 45% specificity) and 75% with CNN (100% sensitivity and 50% specificity). This study demonstrates remarkably accurate diagnosis of breast cancer using AI tools, which significantly improved diagnostic efficacy over conventional statistical methods. On the other hand, the electronic nose prototype employing commercially

available, poorly specific sensors could not compare to GC-MS; despite the efficacy of AI tools without clear biomarkers, it likely needs to be paired with highly specific, targeted sensors to achieve better performance as a clinical diagnostic tool.

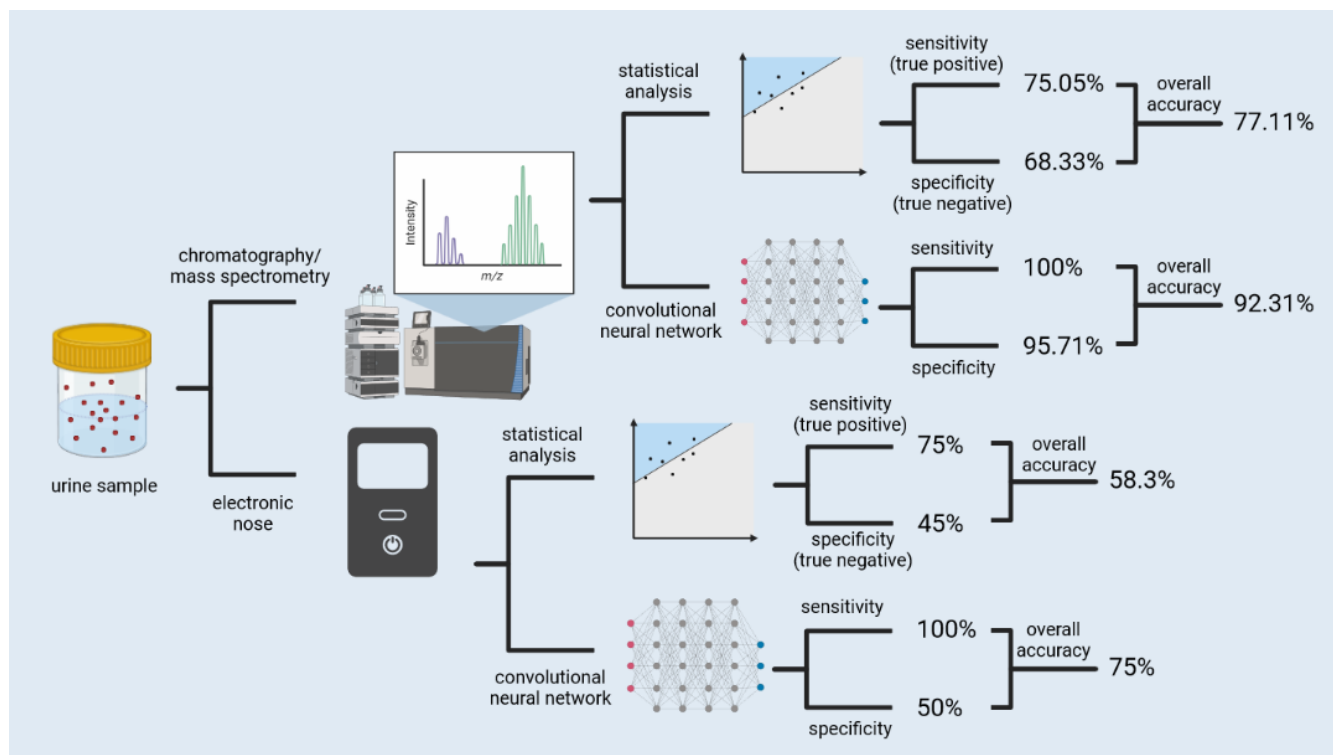


Figure 6. Benet et al. performed a factorial study comparing the diagnostic accuracy of chromatography/mass spectrometry against an electronic nose, and conventional statistical analysis against a convolutional neural network. Perhaps unsurprisingly, the electronic nose demonstrated poor specificity compared with chromatography, but AI pattern recognition proved highly effective compared with statistical tools using the same data [131].

Fu et al. developed an artificially intelligent olfactory (AIO) system as a first attempt at detecting PD with a small-size sensor with classification via machine learning algorithms [120]. The AIO system consists of three modules: (1) sample gas preconcentration in an adsorption tube; (2) separation via gas chromatography (GC); (3) a surface acoustic wave (SAW) sensor to detect mass loading of separated compounds, with embedded machine learning to classify samples based on features. For comparison, the group first applied statistical methods to identify VOC peaks of significant difference between PD patients and controls, as was performed in previous studies [121,122]. The peaks corresponded to perillic aldehyde, octanal, and hexyl acetate. Based on these markers, they achieved a classification accuracy of 70.8% (91.7% sensitivity and 50% specificity, AUC of 0.646). On the other hand, the group trained six ML models employing different strategies on a dataset of 31 PD patients and 32 controls. They tested the models on odor profiles of the remaining 12 PD patients and 12 controls collected during the study. The highest classification accuracies were achieved with ensemble-learning algorithms including random forest at 79.2% (91.7% sensitivity and 66.7% specificity, AUC of 0.868) and Adaboost at 75% (83.3% sensitivity and 66.7% specificity, AUC of 0.929). Despite limitations due to the study's sample size and composition, it shows significant accuracy in PD diagnosis with just three biomarkers. Moreover, the ML algorithms further improved diagnostic accuracy, indicating that insignificant peaks on the chromatogram were also picked up, and contributed to higher classification accuracy. Finally, detection with a SAW sensor is a step towards faster and low-cost analysis compared with GC-MS.

Additional Potential Impacts of Artificial Intelligence

AI may also inspire new innovative designs in olfactory chemosensors. Wang et al. trained an artificial neural network (ANN) to classify simulated odors and found that the resulting neural network took on a structure reminiscent of natural olfactory systems in flies and mice (Figure 7) [132]. The fly and mouse olfactory systems are structured as follows: (1) sensory neurons express a single type of odor receptor; (2) like sensory neurons expressing the same receptor converge at a locus of projection neurons, known as the glomerulus; (3) downstream of the glomerulus, signals diverge into separate neural circuits responsible for innate behaviors and learned behaviors. In the study, the group began with a neural network featuring random, all-to-all connectivity. They trained the network using a million randomly generated odor samples, which were represented by unique odor receptor activation patterns, and accordingly assigned to 100 classes. The training altered connectivity and connection weights, and the result was a network that replicated the three key features of olfactory systems as outlined above. Moreover, some parameters closely matched those in an adult fly, such as each Kenyon cell receiving input from six projection neurons on average. Considering the results of the computational study, and convergently evolved olfactory systems in evolutionarily distant species, the three-layer, input-convergence-expansion structure reflects an underlying logic that may be useful in designing biomimetic olfactory systems.

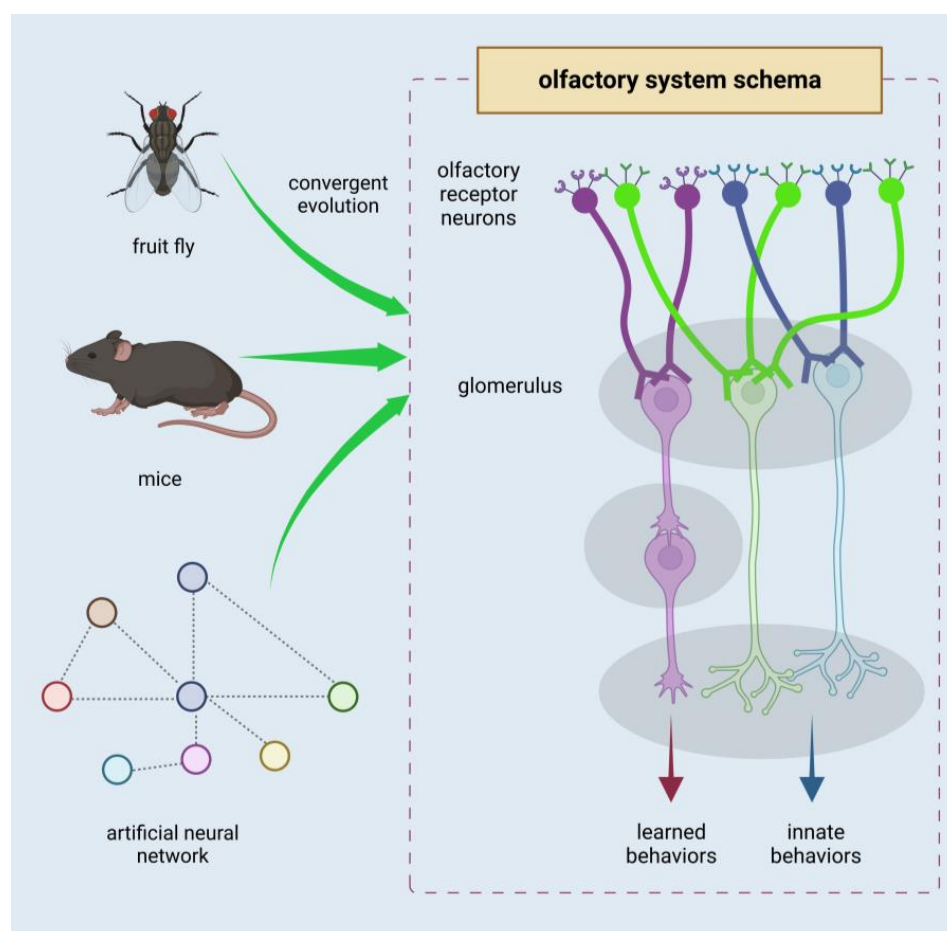


Figure 7. Fruit fly and mouse olfactory systems have very similar structure, with distinctive features including one-to-one mapping between olfactory receptors, receptor neurons, and projection neurons, and separate signal transduction pathways for innate and learned behaviors. Evidently, these systems evolved convergently. Wang et al. demonstrated another instance of such convergent evolution while training an initially random artificial neural network for olfactory classification tasks [81]. Could there be an underlying logic optimal for olfactory sensing?

5. Perspectives

Chemosensing of disease has been gaining traction as more volatile metabolites are discovered to concomitantly appear with disease onset. Chemosensing diagnostics is attractive because it works with noninvasive samples such as breath, saliva, and urine, and the volatile metabolites appear in early stages of disease, which is crucial because early diagnosis leads to significant improvements in patient outcomes. In Section 2, we reviewed recent chemosensing developments towards identifying VOC biomarkers of various cancers of the bladder and lung. We also summarized the emerging concept of analyzing VOCs from sebum to find biomarkers of Parkinson's disease pioneered by Barran's group. In Section 3, we reviewed parallel developments of nanoarchitectonic chemosensors, which demonstrate the potential to yield diagnostic performances comparable to or exceeding the established chemosensing methodology (GC-MS and adjacent technologies). Throughout Sections 2 and 3, the prominent role of AI in recent literature is evident, and we bring the topic center-stage in Section 4, as we delve deeper into the use of AI pattern recognition to analyze biomarker data, how it compares with conventional statistical tools, and the prospective potential for finding optimal structure and operational logic for chemosensing and molecular recognition tasks.

New methodologies for disease diagnosis are actively being developed, and the field is experiencing an unprecedented boom from integrating AI methodologies. The studies we reviewed have demonstrated a powerful synergy between AI diagnostic tools and highly selective and sensitive sensors, as exemplified in the work of Jian et al. [130]. On the other hand, our review also highlights a pressing need for parallel advancements in sensing technology, which are necessary to keep up with and enable the efficiencies brought by AI technology, as demonstrated in the work of Benet et al. [131]. More specifically, advancements in sensor membranes as sensing interfaces and more innovative sensor structures are critical to the current course of development, making them essentially necessary in the near future. Further progress on the materials side of development, coupled with new methodologies, would significantly accelerate the development of chemosensing technology for disease detection and monitoring. This is where nanoarchitectonics, the concept of assembling materials and structures, could make major contributions.

Besides applications in diagnosing cancer and Parkinson's disease as focally depicted in our review, the powerful combination of nanoarchitectonic chemosensors and AI is widely applicable to other diseases that cause metabolic changes. One example that comes to mind is infectious diseases, the monitoring with chemosensing of which has been proposed before, and may be due for an imminent resurgence [133,134]. Along this line of thought, targets for biotechnology and disease countermeasures will be particularly diverse, as new diseases and viruses are continuously emerging. In this case, adaptability of detection membranes and sensing systems would be key, as different pathologies will levy different healthcare demands. A unified methodology is desirable to respond effectively to such future crises.

The most effective approach could derive from the combination of nanoarchitectonics and AI. Nanoarchitectonics can be thought of as the method for everything in materials science. It is a methodology that can be used to create a wide variety of materials. The various sensing structure fabrication methods that nanoarchitectonics provides, and the boons of AI analysis (including pattern recognition, trend identification, decision making, and even proposal of new nanoarchitectonics methods) will arise to address a wide variety of emerging challenges.

In particular, nanoarchitectonics integrates processes such as self-assembly based on artificially manipulated equilibrium and nonequilibrium processes [135,136], which is effective for forming hierarchical structures [137,138]. Since biomolecular recognition and biological reaction processes depend on hierarchical structures, this property of nanoarchitectonics is advantageous for biodetection and diagnosis. In addition, nanoarchitectonics can benefit from synergy with uncertain phenomena such as thermal fluctuations in the formation of structures [139,140]; this feature is also suitable for application to biosystems,

which innately operate with thermal fluctuations. The combination of supramolecular organization through nanoarchitectonics and microfabrication techniques for device structures would also be very useful for creating advanced sensors. These will give rise to many options, and AI technologies will help optimize and streamline them. Disease diagnosis and detection of emerging viruses are important challenges facing society. The arsenal of solutions and relevant methodologies advances day by day, including the use of AI. Nevertheless, technologies such as advanced functional membranes for diverse targets need to be developed in lockstep to support and enable emergent software advancements. The material and structural formative technologies of nanoarchitectonics will be required to meet these challenges.

Author Contributions: Descriptions of and discussions on diagnostic examples were mainly made by X.S., and backgrounds and perspectives were mainly described by K.A. All authors have read and agreed to the published version of the manuscript.

Funding: This study was partially supported by JSPS KAKENHI grant number JP20H00392 and JP23H05459.

Conflicts of Interest: The authors declare no conflict of interest.

References

1. Guo, D.; Shibuya, R.; Akiba, C.; Saji, S.; Kondo, T.; Nakamura, J. Active sites of nitrogen-doped carbon materials for oxygen reduction reaction clarified using model catalysts. *Science* **2016**, *351*, 361–365. [[CrossRef](#)] [[PubMed](#)]
2. Maeda, K.; Takeiri, F.; Kobayashi, G.; Matsuiishi, S.; Ogino, H.; Ida, S.; Mori, T.; Uchimoto, Y.; Tanabe, S.; Hasegawa, T.; et al. Recent progress on mixed-anion materials for energy applications. *Bull. Chem. Soc. Jpn.* **2022**, *95*, 26–37. [[CrossRef](#)]
3. Yoshino, A. The lithium-ion battery: Two breakthroughs in development and two reasons for the Nobel prize. *Bull. Chem. Soc. Jpn.* **2022**, *95*, 195–197. [[CrossRef](#)]
4. Chen, G.; Singh, S.K.; Takeyasu, K.; Hill, J.P.; Nakamura, J.; Ariga, K. Versatile nanoarchitectonics of Pt with morphology control of oxygen reduction reaction catalysts. *Sci. Technol. Adv. Mater.* **2022**, *23*, 413–423. [[CrossRef](#)]
5. Hosaka, T.; Komaba, S. Development of nonaqueous electrolytes for high-voltage K-ion batteries. *Bull. Chem. Soc. Jpn.* **2022**, *95*, 569–581. [[CrossRef](#)]
6. Saidul Islam, M.S.; Shudo, Y.; Hayami, S. Energy conversion and storage in fuel cells and super-capacitors from chemical modifications of carbon allotropes: State-of-art and prospect. *Bull. Chem. Soc. Jpn.* **2022**, *95*, 1–25. [[CrossRef](#)]
7. Klyndyuk, A.I.; Chizhova, E.A.; Kharytonau, D.S.; Medvedev, D.A. Layered oxygen-deficient double perovskites as promising cathode materials for solid oxide fuel cells. *Materials* **2022**, *15*, 141. [[CrossRef](#)]
8. Kinoshita, T. Highly efficient wideband solar energy conversion employing singlet-triplet transitions. *Bull. Chem. Soc. Jpn.* **2022**, *95*, 341–352. [[CrossRef](#)]
9. Jakhar, M.; Kumar, A.; Ahluwalia, P.K.; Tankeshwar, K.; Pandey, R. Engineering 2D materials for photocatalytic water-splitting from a theoretical perspective. *Materials* **2022**, *15*, 2221. [[CrossRef](#)]
10. Nguyen, M.T.; Muramatsu, T.; Kheawhom, S.; Wattanakit, C.; Yonezawa, T. Impact of morphology and transition metal doping of vanadate nanowires without surface modification on the performance of aqueous zinc-ion batteries. *Bull. Chem. Soc. Jpn.* **2022**, *95*, 728–734. [[CrossRef](#)]
11. Mori, H.; Yamada, Y.; Minagawa, Y.; Hasegawa, N.; Nishihara, Y. Effects of acyloxy groups in anthrabi-thiadiazole-based semiconducting polymers on electronic properties, thin-film structure, and solar cell performance. *Bull. Chem. Soc. Jpn.* **2022**, *95*, 942–952. [[CrossRef](#)]
12. Pastuszak, J.; Węgierek, P. Photovoltaic cell generations and current research directions for their development. *Materials* **2022**, *15*, 5542. [[CrossRef](#)]
13. Charles-Blin, Y.; Kondo, T.; Wu, Y.; Bandow, S.; Awaga, K. Salt-assisted pyrolysis of covalent organic framework for controlled active nitrogen functionalities for oxygen reduction reaction. *Bull. Chem. Soc. Jpn.* **2022**, *95*, 972–977. [[CrossRef](#)]
14. Murugan, S.; Lee, E.-C. Recent Advances in the synthesis and application of vacancy-ordered halide double perovskite materials for solar cells: A promising alternative to lead-based perovskites. *Materials* **2023**, *16*, 5275. [[CrossRef](#)] [[PubMed](#)]
15. Desoky, M.M.H.; Caldera, F.; Brunella, V.; Ferrero, R.; Hoti, G.; Trotta, F. Cyclodextrins for lithium batteries applications. *Materials* **2023**, *16*, 5540. [[CrossRef](#)] [[PubMed](#)]
16. Honda, M.; Suzuki, N. Toxicities of polycyclic aromatic hydrocarbons for aquatic animals. *Int. J. Environ. Res. Public Health* **2020**, *17*, 41363. [[CrossRef](#)]
17. Boukhalfa, N.; Darder, M.; Boutahala, M.; Aranda, P.; Ruiz-Hitzky, E. Composite nanoarchitectonics: Alginate beads encapsulating Sepiolite/magnetite/Prussian blue for removal of cesium ions from water. *Bull. Chem. Soc. Jpn.* **2021**, *94*, 122–132. [[CrossRef](#)]

18. Singh, G.; Lee, J.M.; Kothandam, G.; Palanisami, T.; Al-Muhtaseb, A.H.; Karakoti, A.; Yi, J.; Bolan, N.; Vinu, A. A review on the synthesis and applications of nanoporous carbons for the removal of complex chemical contaminants. *Bull. Chem. Soc. Jpn.* **2021**, *94*, 1232–1257. [[CrossRef](#)]
19. Chen, S.; Liu, J.; Zhang, Q.; Teng, F.; McLellan, B.C. A critical review on deployment planning and risk analysis of carbon capture, utilization, and storage (CCUS) toward carbon neutrality. *Renew. Sus. Energy Rev.* **2022**, *167*, 112537. [[CrossRef](#)]
20. Chapman, A.; Ertekin, E.; Kubota, M.; Nagao, A.; Bertsch, K.; Macadre, A.; Tsuchiyama, T.; Masamura, T.; Takaki, S.; Komoda, R.; et al. Achieving a carbon neutral future through advanced functional materials and technologies. *Bull. Chem. Soc. Jpn.* **2022**, *95*, 73–103. [[CrossRef](#)]
21. Sasai, R.; Fujimura, T.; Sato, H.; Nii, E.; Sugata, M.; Nakayashiki, Y.; Hoashi, H.; Moriyoshi, C.; Oishi, E.; Fujii, Y.; et al. Origin of selective nitrate removal by Ni²⁺–Al³⁺ layered double hydroxides in aqueous media and its application potential in seawater purification. *Bull. Chem. Soc. Jpn.* **2022**, *95*, 802–812. [[CrossRef](#)]
22. Qaidi, S.; Najm, H.M.; Abed, S.M.; Özkılıç, Y.O.; Al Dughaihi, H.; Alost, M.; Sabri, M.M.S.; Alkhatib, F.; Milad, A. Concrete containing waste glass as an environmentally friendly aggregate: A review on fresh and mechanical characteristics. *Materials* **2022**, *15*, 6222. [[CrossRef](#)] [[PubMed](#)]
23. Yagyu, J.; Islam, M.S.; Yasutake, H.; Hirayama, H.; Zenno, H.; Sugimoto, A.; Takagi, S.; Sekine, Y.; Ohira, S.; Hayami, S. Insights and further understanding of radioactive cesium removal using zeolite, Prussian blue and graphene oxide as adsorbents. *Bull. Chem. Soc. Jpn.* **2022**, *95*, 862–870. [[CrossRef](#)]
24. Gupta, V.; Biswas, D.; Roy, S. A comprehensive review of biodegradable polymer-based films and coatings and their food packaging applications. *Materials* **2022**, *15*, 5899. [[CrossRef](#)]
25. Ren, F.; He, R.; Ren, J.; Tao, F.; Yang, H.; Lv, H.; Ju, X. A friendly UV-responsive fluorine-free superhydrophobic coating for oil-water separation and dye degradation. *Bull. Chem. Soc. Jpn.* **2022**, *95*, 1091–1099. [[CrossRef](#)]
26. Purchase, C.K.; Al Zulayq, D.M.; O'Brien, B.T.; Kowalewski, M.J.; Berenjian, A.; Tarighaleslami, A.H.; Seifan, M. Circular economy of construction and demolition waste: A literature review on lessons, challenges, and benefits. *Materials* **2022**, *15*, 76. [[CrossRef](#)]
27. Mamun, M.R.A.; Yusuf, M.A.; Bhuyan, M.M.; Bhuiyan, M.S.H.; Arafath, M.A.; Uddin, M.N.; Soeb, M.J.A.; Almahri, A.; Rahman, M.M.; Karim, M.R. Acidity controlled desulfurization of biogas by using iron (III) and ferrosferic (II, III) oxide. *Bull. Chem. Soc. Jpn.* **2022**, *95*, 1234–1241. [[CrossRef](#)]
28. Han, X.; Wang, S.; Liu, M.; Liu, L. A cucurbit[6]uril-based supramolecular assembly as a multifunctional material for the detection and removal of organic explosives and antibiotics. *Bull. Chem. Soc. Jpn.* **2022**, *95*, 1445–1452. [[CrossRef](#)]
29. Marczak, D.; Lejcuś, K.; Lejcuś, I.; Misiewicz, J. Sustainable innovation: Turning waste into soil additives. *Materials* **2023**, *16*, 2900. [[CrossRef](#)]
30. Simonenko, N.P.; Glukhova, O.E.; Plugin, I.A.; Kolosov, D.A.; Nagornov, I.A.; Simonenko, T.L.; Varezchnikov, A.S.; Simonenko, E.P.; Sysoev, V.V.; Kuznetsov, N.T. The Ti0.2V1.8C MXene ink-prepared chemiresistor: From theory to tests with humidity versus VOCs. *Chemosensors* **2023**, *11*, 7. [[CrossRef](#)]
31. Chowdhury, R.; Al Biruni, M.T.; Afia, A.; Hasan, M.; Islam, M.R.; Ahmed, T. Medical waste incineration fly ash as a mineral filler in dense bituminous course in flexible pavements. *Materials* **2023**, *16*, 5612. [[CrossRef](#)] [[PubMed](#)]
32. Cabral, H.; Miyata, K.; Osada, K.; Kataoka, K. Block copolymer micelles in nanomedicine applications. *Chem. Rev.* **2018**, *118*, 6844–6892. [[CrossRef](#)] [[PubMed](#)]
33. Li, J.; Kataoka, K. Chemo-physical strategies to advance the in vivo functionality of targeted nanomedicine: The next generation. *J. Am. Chem. Soc.* **2021**, *143*, 538–559. [[CrossRef](#)]
34. Fujita, Y.; Niizeki, T.; Fukumitsu, N.; Ariga, K.; Yamauchi, Y.; Malgras, V.; Kaneti, Y.V.; Liu, C.-H.; Hatano, K.; Suematsu, H.; et al. Mechanisms responsible for adsorption of molybdate ions on alumina for the production of medical radioisotopes. *Bull. Chem. Soc. Jpn.* **2022**, *95*, 129–137. [[CrossRef](#)]
35. Quader, S.; Kataoka, K.; Cabral, H. Nanomedicine for brain cancer. *Adv. Drug Deliv. Rev.* **2022**, *182*, 114115. [[CrossRef](#)]
36. Komiyama, M. Molecular mechanisms of the medicines for COVID-19. *Bull. Chem. Soc. Jpn.* **2022**, *95*, 1308–1317. [[CrossRef](#)]
37. Tiburcius, S.; Krishnan, K.; Patel, V.; Netherton, J.; Sathish, C.L.; Weidenhofer, J.; Yang, J.-H.; Verrills, N.M.; Karakoti, A.; Vinu, A. Triple surfactant assisted synthesis of novel core-shell mesoporous silica nanoparticles with high surface area for drug delivery for prostate cancer. *Bull. Chem. Soc. Jpn.* **2022**, *95*, 331–340. [[CrossRef](#)]
38. Islam, F.; Shohag, S.; Uddin, M.J.; Islam, M.R.; Nafady, M.H.; Akter, A.; Mitra, S.; Roy, A.; Emran, T.B.; Cavalu, S. Exploring the journey of zinc oxide nanoparticles (ZnO-NPs) toward biomedical applications. *Materials* **2022**, *15*, 2160. [[CrossRef](#)]
39. Pradipta, A.R.; Michiba, H.; Kubo, A.; Fujii, M.; Tanei, T.; Morimoto, K.; Shimazu, K.; Tanaka, K. The second-generation click-to-sense probe for intraoperative diagnosis of breast cancer tissues based on acrolein targeting. *Bull. Chem. Soc. Jpn.* **2022**, *95*, 421–426. [[CrossRef](#)]
40. Musielak, E.; Feliczak-Guzik, A.; Nowak, I. Synthesis and potential applications of lipid nanoparticles in medicine. *Materials* **2022**, *15*, 682. [[CrossRef](#)]
41. Su, C.-H.; Soendoro, A.; Okayama, S.; Rahmania, F.J.; Nagai, T.; Imae, T.; Tsutsumiuchi, K.; Kawai, N. Drug release stimulated by magnetic field and light on magnetite- and carbon dot-loaded carbon nanohorn. *Bull. Chem. Soc. Jpn.* **2022**, *95*, 582–594. [[CrossRef](#)]
42. Lvov, V.A.; Senatov, F.S.; Veveris, A.A.; Skrybykina, V.A.; Díaz Lantada, A. Auxetic metamaterials for biomedical devices: Current situation, main challenges, and research trends. *Materials* **2022**, *15*, 1439. [[CrossRef](#)] [[PubMed](#)]

43. Sahayasheela, V.J.; Yu, Z.; Hirose, Y.; Pandian, G.N.; Bando, T.; Sugiyama, H. Inhibition of GLI-mediated transcription by cyclic pyrrole-imidazole polyamide in cancer stem cells. *Bull. Chem. Soc. Jpn.* **2022**, *95*, 693–699. [[CrossRef](#)]
44. Fu, H.; Xu, Z.; Hou, H.; Luo, R.; Ju, H.; Lei, J. Framework-enhanced electrochemiluminescence in biosensing. *Chemosensors* **2023**, *11*, 422. [[CrossRef](#)]
45. Larasati, L.; Lestari, W.W.; Firdaus, M. Dual-action Pt(IV) prodrugs and targeted delivery in metal-organic frameworks: Overcoming cisplatin resistance and improving anticancer activity. *Bull. Chem. Soc. Jpn.* **2022**, *95*, 1561–1577. [[CrossRef](#)]
46. Ghilan, A.; Nicu, R.; Ciolacu, D.E.; Ciolacu, F. Insight into the latest medical applications of nanocellulose. *Materials* **2023**, *16*, 4447. [[CrossRef](#)]
47. Baranwal, J.; Barse, B.; Di Petrillo, A.; Gatto, G.; Pilia, L.; Kumar, A. Nanoparticles in cancer diagnosis and treatment. *Materials* **2023**, *16*, 5354. [[CrossRef](#)] [[PubMed](#)]
48. Sugimoto, Y.; Pou, P.; Abe, M.; Jelinek, P.; Pérez, R.; Morita, S.; Custance, Ó. Chemical identification of individual surface atoms by atomic force microscopy. *Nature* **2007**, *446*, 64–67. [[CrossRef](#)]
49. Kimura, K.; Miwa, K.; Imada, H.; Imai-Imada, M.; Kawahara, S.; Takeya, J.; Kawai, M.; Galperin, M.; Kim, Y. Selective triplet exciton formation in a single molecule. *Nature* **2019**, *570*, 210–213. [[CrossRef](#)]
50. Harano, K. Self-assembly mechanism in nucleation processes of molecular crystalline materials. *Bull. Chem. Soc. Jpn.* **2021**, *94*, 463–472. [[CrossRef](#)]
51. Bacilla, A.C.C.; Okada, Y.; Yoshimoto, S.; Islyaikin, M.K.; Koifman, O.I.; Nagao Kobayashi, N. Triangular expanded hemiporphyrines: Electronic structures and nanoscale characterization of their adlayers on Au(111). *Bull. Chem. Soc. Jpn.* **2021**, *94*, 34–43. [[CrossRef](#)]
52. Ishikawa, T.; Noguchi, M.; Kato, K.; Kuramori, M.; Narita, T.; Oishi, Y. Maze pattern at nanometer-scale in a mixed Langmuir monolayer of fatty acids. *Bull. Chem. Soc. Jpn.* **2021**, *94*, 2967–2969. [[CrossRef](#)]
53. Bhattacharya, T.; Soares, G.A.B.e.; Chopra, H.; Rahman, M.M.; Hasan, Z.; Swain, S.S.; Cavalu, S. Applications of phyto-nanotechnology for the treatment of neurodegenerative disorders. *Materials* **2022**, *15*, 804. [[CrossRef](#)]
54. Tokoro, H.; Nakabayashi, K.; Nagashima, S.; Song, Q.; Yoshikiyo, M.; Ohkoshi, S. Optical properties of epsilon Iron oxide nanoparticles in the millimeter- and terahertz-wave regions. *Bull. Chem. Soc. Jpn.* **2022**, *95*, 538–552. [[CrossRef](#)]
55. Markandan, K.; Chai, W.S. Perspectives on nanomaterials and nanotechnology for sustainable bioenergy generation. *Materials* **2022**, *15*, 7769. [[CrossRef](#)]
56. Kameda, Y.; Kowaguchi, M.; Amo, Y.; Usuki, T.; Okuyama, D.; Sato, T.J. Experimental determination of deviation from spherical electron densities of atoms in benzene molecules in the liquid state. *Bull. Chem. Soc. Jpn.* **2022**, *95*, 1680–1686. [[CrossRef](#)]
57. Mikšić Trontl, V.; Jedovnicki, I.; Pervan, P. STM study of the initial stage of gold intercalation of graphene on Ir(111). *Materials* **2023**, *16*, 3833. [[CrossRef](#)]
58. Kawawaki, T.; Shimizu, N.; Mitomi, Y.; Yazaki, D.; Hossain, S.; Negishi, Y. Supported, ~1-nm-sized platinum clusters: Controlled preparation and enhanced catalytic activity. *Bull. Chem. Soc. Jpn.* **2021**, *94*, 2853–2870. [[CrossRef](#)]
59. Ariga, K.; Li, M.; Richards, G.J.; Hill, J.P. Nanoarchitectonics: A conceptual paradigm for design and synthesis of dimension-controlled functional nanomaterials. *J. Nanosci. Nanotechnol.* **2011**, *11*, 1–13. [[CrossRef](#)]
60. Ariga, K.; Ji, Q.; Nakanishi, W.; Hill, J.P.; Aono, M. Nanoarchitectonics: A new materials horizon for nanotechnolog. *Mater. Horiz.* **2015**, *2*, 406–413. [[CrossRef](#)]
61. Ariga, K. Nanoarchitectonics: What's coming next after nanotechnology? *Nanoscale Horiz.* **2021**, *6*, 364–378. [[CrossRef](#)]
62. Feynman, R.P. There's plenty of room at the bottom. *California Inst. Technol. J. Eng. Sci.* **1960**, *4*, 23–36.
63. Roukes, M. Plenty of room, indeed. *Sci. Am.* **2001**, *285*, 48–57. [[CrossRef](#)] [[PubMed](#)]
64. Ariga, K.; Minami, K.; Ebara, M.; Nakanishi, J. What are the emerging concepts and challenges in NANO? Nanoarchitectonics, hand-operating nanotechnology and mechanobiology. *Polym. J.* **2016**, *48*, 371–389. [[CrossRef](#)]
65. Tsuchiya, T.; Nakayama, T.; Ariga, K. Nanoarchitectonics Intelligence with atomic switch and neuromorphic network system. *Appl. Phys. Express* **2022**, *15*, 100101. [[CrossRef](#)]
66. Ariga, K.; Li, J.; Fei, J.; Ji, Q.; Hill, J.P. Nanoarchitectonics for dynamic functional materials from atomic-/molecular-level manipulation to macroscopic action. *Adv. Mater.* **2016**, *28*, 1251–1286. [[CrossRef](#)] [[PubMed](#)]
67. Ariga, K.; Shionoya, M. Nanoarchitectonics for coordination asymmetry and related chemistry. *Bull. Chem. Soc. Jpn.* **2021**, *94*, 839–859. [[CrossRef](#)]
68. Ariga, K. Materials nanoarchitectonics in a two-dimensional world within a nanoscale distance from the liquid phase. *Nanoscale* **2022**, *14*, 10610–10629. [[CrossRef](#)]
69. Laughlin, R.B.; Pines, D. The theory of everything. *Proc. Natl. Acad. Sci. USA* **2000**, *97*, 28–31. [[CrossRef](#)]
70. Ariga, K.; Fakhrullin, R. Materials nanoarchitectonics from atom to living cell: A method for everything. *Bull. Chem. Soc. Jpn.* **2022**, *95*, 774–795. [[CrossRef](#)]
71. Wu, S.; Kondo, Y.; Kakimoto, M.; Yang, B.; Yamada, H.; Kuwajima, I.; Lambard, G.; Hongo, K.; Xu, Y.; Shiomi, J.; et al. Machine-learning-assisted discovery of polymers with high thermal conductivity using a molecular design algorithm. *Npj Comput. Mater.* **2019**, *5*, 66. [[CrossRef](#)]
72. Toyao, T.; Maeno, Z.; Takakusagi, S.; Kamachi, T.; Takigawa, I.; Shimizu, K. Machine learning for catalysis informatics: Recent applications and prospect. *ACS Catal.* **2020**, *10*, 2260–2297. [[CrossRef](#)]

73. Neto, M.P.; Soares, A.C.; Oliveira, O.N., Jr.; Paulovich, F.V. Machine learning used to create a multidimensional calibration space for sensing and biosensing data. *Bull. Chem. Soc. Jpn.* **2021**, *94*, 1553–1562. [[CrossRef](#)]
74. Yuan, X.; Tian, Y.; Ahmad, W.; Ahmad, A.; Usanova, K.I.; Mohamed, A.M.; Khallaf, R. Machine learning prediction models to evaluate the strength of recycled aggregate concrete. *Materials* **2022**, *15*, 2823. [[CrossRef](#)] [[PubMed](#)]
75. Sadoun, A.M.; Najjar, I.R.; AlSORUJI, G.S.; Abd-Elwahed, M.S.; Elaziz, M.A.; Fathy, A. Utilization of improved machine learning method based on artificial hummingbird algorithm to predict the tribological behavior of Cu-Al₂O₃ nanocomposites synthesized by in situ method. *Mathematics* **2022**, *10*, 1266. [[CrossRef](#)]
76. Shang, M.; Li, H.; Ahmad, A.; Ahmad, W.; Ostrowski, K.A.; Aslam, F.; Joyklad, P.; Majka, T.M. Predicting the mechanical properties of RCA-based concrete using supervised machine learning algorithms. *Materials* **2022**, *15*, 647. [[CrossRef](#)]
77. Wang, J.; Ghosh, D.B.; Zhang, Z. Computational materials design for ceramic Nuclear waste forms using machine learning, First-principles calculations, and kinetics rate theory. *Materials* **2023**, *16*, 4985. [[CrossRef](#)]
78. Champa-Bujaico, E.; Díez-Pascual, A.M.; García-Díaz, P. Synthesis and characterization of polyhydroxyalkanoate/graphene oxide/nanoclay bionanocomposites: Experimental results and theoretical predictions via machine learning models. *Biomolecules* **2023**, *13*, 1192. [[CrossRef](#)]
79. Agrawal, A.; Choudhary, A. Perspective: Materials informatics and big data: Realization of the “fourth paradigm” of science in materials science. *APL Mater* **2016**, *4*, 053208. [[CrossRef](#)]
80. Ramprasad, R.; Batra, R.; Paliania, G.; Kanakithodi, A.M.; Kim, C. Machine learning in materials informatics: Recent applications and prospects. *npj Comput. Mater.* **2017**, *3*, 54. [[CrossRef](#)]
81. Oaki, Y.; Igarashi, Y. Materials informatics for 2D materials combined with sparse modeling and chemical perspective: Toward small-data-driven chemistry and materials science. *Bull. Chem. Soc. Jpn.* **2021**, *94*, 2410–2422. [[CrossRef](#)]
82. Venkatraman, V.; Alsberg, B.K. Designing high-refractive index polymers using materials informatics. *Polymers* **2018**, *10*, 103. [[CrossRef](#)] [[PubMed](#)]
83. Frydrych, K.; Karimi, K.; Pecelerowicz, M.; Alvarez, R.; Dominguez-Gutiérrez, F.J.; Rovaris, F.; Papanikolaou, S. Materials informatics for mechanical deformation: A review of applications and challenges. *Materials* **2021**, *14*, 5764. [[CrossRef](#)] [[PubMed](#)]
84. Matsumoto, F.; Sumino, S.; Iwai, T.; Takatoshi Ito, T. Design of linearly substituted fullerene bis-adducts with high dielectric constants based on theoretical calculations. *Bull. Chem. Soc. Jpn.* **2021**, *94*, 1833–1839. [[CrossRef](#)]
85. Hayakawa, M.; Sakano, K.; Kumada, K.; Tobita, H.; Igarashi, Y.; Citterio, D.; Oaki, Y.; Hiruta, Y. Development of prediction model for cloud point of thermo-responsive polymers by experiment-oriented materials informatics. *Polym. Chem.* **2023**, *14*, 2383–2389. [[CrossRef](#)]
86. Hatakeyama-Sato, K.; Umeki, M.; Adachi, H.; Kuwata, N.; Hasegawa, G.; Kenichi Oyaizu, K. Exploration of organic superionic glassy conductors by process and materials informatics with lossless graph database. *Npj Comput. Mater.* **2011**, *8*, 170. [[CrossRef](#)]
87. Hara, K.; Yamada, S.; Kurotani, A.; Chikayama, E.; Kikuchi, J. Materials informatics approach using domain modelling for exploring structure–property relationships of polymers. *Sci. Rep.* **2022**, *12*, 10558. [[CrossRef](#)]
88. Chaikittisilp, W.; Yamauchi, Y.; Ariga, K. Material evolution with nanotechnology, nanoarchitectonics, and materials informatics: What will be the next paradigm shift in nanoporous materials? *Adv. Mater.* **2022**, *34*, 2107212. [[CrossRef](#)]
89. Nakanishi, W.; Minami, K.; Shrestha, L.K.; Ji, Q.; Hill, J.P.; Ariga, K. Bioactive nanocarbon assemblies: Nanoarchitectonics and applications. *Nano Today* **2014**, *9*, 378–394. [[CrossRef](#)]
90. Shen, X.; Song, J.; Sevencan, C.; Leong, D.T.; Ariga, K. Bio-interactive nanoarchitectonics with two-dimensional materials and environments. *Sci. Technol. Adv. Mater.* **2022**, *23*, 199–224. [[CrossRef](#)]
91. Chang, R.; Zhao, L.; Xing, R.; Li, J.; Yan, X. Functional chromopeptide nanoarchitectonics: Molecular design, self-assembly and biological applications. *Chem. Soc. Rev.* **2023**, *52*, 2688–2712. [[CrossRef](#)]
92. Jia, X.; Chen, J.; Lv, W.; Li, H.; Ariga, K. Engineering dynamic and interactive biomaterials using material nanoarchitectonics for modulation of cellular behaviors. *Cell Rep. Phys. Sci.* **2023**, *4*, 101251. [[CrossRef](#)]
93. Ariga, K.; Ji, Q.; McShane, M.J.; Lvov, Y.M.; Vinu, A.; Hill, J.P. Inorganic nanoarchitectonics for biological applications. *Chem. Mater.* **2012**, *24*, 728–737. [[CrossRef](#)]
94. Banerjee, S.; Pillai, J. Solid lipid matrix mediated nanoarchitectonics for improved oral bioavailability of drugs. *Expert Opin. Drug Metab. Toxicol.* **2019**, *15*, 499–515. [[CrossRef](#)]
95. Hu, W.; Shi, J.; Lv, W.; Jia, J.; Ariga, K. Regulation of stem cell fate and function by using bioactive materials with nanoarchitectonics for regenerative medicine. *Sci. Technol. Adv. Mater.* **2022**, *23*, 393–412. [[CrossRef](#)]
96. Moradi, R.; Khalili, N.P.; Septiani, N.L.W.; Liu, C.-H.; Doustkhah, E.; Yamauchi, Y.; Rotkin, S.V. Nanoarchitectonics for abused-drug biosensors. *Small* **2022**, *18*, 2104847. [[CrossRef](#)]
97. Ishihara, S.; Labuta, J.; Van Rossom, W.; Ishikawa, D.; Minami, K.; Hill, J.P.; Ariga, K. Porphyrin-based sensor nanoarchitectonics in diverse physical detection modes. *Phys. Chem. Chem. Phys.* **2014**, *16*, 9713–9746. [[CrossRef](#)]
98. Guo, C.; Wang, T. Zigzag direction nanoarchitectonics of monolayer GeSe for SO₂ gas sensors with high sensitivity and selectivity: A first-principles study. *Appl. Phys. A* **2022**, *128*, 975. [[CrossRef](#)]
99. Joshi, V.; Hussain, S.; Dua, S.; Arora, N.; Mir, S.H.; Rydzek, G.; Senthilkumar, T. Oligomer sensor nanoarchitectonics for “turn-on” fluorescence detection of cholesterol at the nanomolar level. *Molecules* **2022**, *27*, 2856. [[CrossRef](#)]

100. Ma, K.; Yang, L.; Liu, J.; Liu, J. Electrochemical sensor nanoarchitectonics for sensitive detection of uric acid in human whole blood based on screen-printed carbon electrode equipped with vertically-ordered mesoporous silica-nanochannel film. *Nanomaterials* **2022**, *12*, 1157. [[CrossRef](#)]
101. Vaghasiya, J.V.; Mayorga-Martinez, C.C.; Pumera, M. Wearable sensors for telehealth based on emerging materials and nanoarchitectonics. *npj Flex Electron.* **2023**, *7*, 26. [[CrossRef](#)] [[PubMed](#)]
102. Liu, J.; Wang, R.; Zhou, H.; Mathesh, M.; Dubey, M.; Zhang, W.; Wang, B.; Yang, W. Nucleic acid isothermal amplification-based soft nanoarchitectonics as an emerging electrochemical biosensing platform. *Nanoscale* **2022**, *14*, 10286–10298. [[CrossRef](#)]
103. Juste-Dolz, A.; Delgado-Pinar, M.; Avella-Oliver, M.; Fernández, E.; Cruz, J.L.; Andrés, M.V.; Maquieira, Á. Denaturing for nanoarchitectonics: Local and periodic UV-laser photodeactivation of protein bilayers to create functional patterns for biosensing. *ACS Appl. Mater. Interfaces* **2022**, *14*, 41640–41648. [[CrossRef](#)] [[PubMed](#)]
104. Muslu, E.; Eren, E.; Oksuz, A.U. Prussian blue-based flexible thin film nanoarchitectonics for non-enzymatic electrochemical glucose sensor. *J. Inorg. Organomet. Polym.* **2022**, *32*, 2843–2852. [[CrossRef](#)]
105. Ashok, A.; Nguyen, T.-K.; Barton, M.; Leitch, M.; Masud, M.K.; Park, H.; Truong, T.-A.; Kaneti, Y.V.; Ta, H.T.; Li, X.; et al. Flexible nanoarchitectonics for biosensing and physiological monitoring applications. *Small* **2023**, *19*, 2204946. [[CrossRef](#)] [[PubMed](#)]
106. Kim, S.; Baek, S.; Sluyter, R.; Konstantinov, K.; Kim, J.H.; Kim, S.; Kim, Y.H. Wearable and implantable bioelectronics as eco-friendly and patient-friendly integrated nanoarchitectonics for next-generation smart healthcare technology. *EcoMat* **2023**, *5*, e12356. [[CrossRef](#)]
107. Bujak, R.; Struck-Lewicka, W.; Markuszewski, M.J.; Kalisz, R. Metabolomics for laboratory diagnostics. *J. Pharm. Biomed. Anal.* **2015**, *113*, 108–120. [[CrossRef](#)]
108. Beale, D.J.; Jones, O.A.H.; Karpe, A.V.; Dayalan, S.; Oh, D.Y.; Kouremenos, K.A.; Ahmed, W.; Palombo, E.A. A review of analytical techniques and their application in disease diagnosis in breathomics and salivaomics research. *Int. J. Mol. Sci.* **2017**, *18*, 10024. [[CrossRef](#)]
109. Strauch, M.; Lüdke, A.; Münch, D.; Laudes, T.; Giovanni Galizia, C.; Martinelli, E.; Lavra, L.; Paolesse, R.; Olivieri, A.; Catini, A.; et al. More than apples and oranges—Detecting cancer with a fruit fly’s antenna. *Sci. Rep.* **2014**, *4*, 3576. [[CrossRef](#)]
110. Farnum, A.; Parnas, M.; Hoque Apu, E.; Cox, E.; Lefevre, N.; Contag, C.H.; Saha, D. Harnessing insect olfactory neural circuits for detecting and discriminating human cancers. *Biosens. Bioelectron.* **2023**, *219*, 114814. [[CrossRef](#)]
111. Pomerantz, A.; Blachman-Braun, R.; Galnares-Olalde, J.A.; Berebichez-Fridman, R.; Capurso-García, M. The possibility of inventing new technologies in the detection of cancer by applying elements of the canine olfactory apparatus. *Med. Hypotheses* **2015**, *85*, 160–172. [[CrossRef](#)] [[PubMed](#)]
112. Pirrone, F.; Albertini, M. Olfactory detection of cancer by trained sniffer dogs: A systematic review of the literature. *J. Vet. Behav.-Clin. Appl. Res.* **2017**, *19*, 105–117. [[CrossRef](#)]
113. Oh, Y.; Kwon, O.S.; Min, S.S.; Shin, Y.B.; Oh, M.K.; Kim, M. Olfactory detection of toluene by detection rats for potential screening of lung cancer. *Sensors* **2021**, *21*, 2967. [[CrossRef](#)]
114. Sani, S.N.; Zhou, W.; Ismail, B.B.; Zhang, Y.; Chen, Z.; Zhang, B.; Bao, C.; Zhang, H.; Wang, X. LC-MS/MS Based volatile organic compound biomarkers analysis for early detection of lung cancer. *Cancers* **2023**, *15*, 1186. [[CrossRef](#)] [[PubMed](#)]
115. Wang, P.; Huang, Q.; Meng, S.; Mu, T.; Liu, Z.; He, M.; Li, Q.; Zhao, S.; Wang, S.; Qiu, M. Identification of lung cancer breath biomarkers based on perioperative breathomics testing: A prospective observational study. *eClinicalMedicine* **2022**, *47*, 101384. [[CrossRef](#)]
116. Ligor, T.; Adamczyk, P.; Kowalkowski, T.; Ratiu, I.A.; Wenda-Piesik, A.; Buszewski, B. Analysis of VOCs in urine samples directed towards bladder cancer detection. *Molecules* **2022**, *27*, 5023. [[CrossRef](#)]
117. Rietcheck, H.R.; Maghfour, J.; Rundle, C.W.; Husayn, S.S.; Presley, C.L.; Sillau, S.H.; Liu, Y.; Leehey, M.A.; Dunnick, C.A.; Dellavalle, R.P. A review of the current evidence connecting seborrheic dermatitis and Parkinson’s disease and the potential role of oral cannabinoids. *Dermatology* **2021**, *237*, 872–877. [[CrossRef](#)]
118. Sinclair, E.; Trivedi, D.K.; Sarkar, D.; Walton-Doyle, C.; Milne, J.; Kunath, T.; Rijs, A.M.; de Bie, R.M.A.; Goodacre, R.; Silverdale, M.; et al. Metabolomics of sebum reveals lipid dysregulation in Parkinson’s disease. *Nat. Commun.* **2021**, *12*, 1592. [[CrossRef](#)]
119. Sarkar, D.; Sinclair, E.; Lim, S.H.; Walton-Doyle, C.; Jafri, K.; Milne, J.; Vissers, J.P.C.; Richardson, K.; Trivedi, D.K.; Silverdale, M.; et al. Paper spray ionization ion mobility mass spectrometry of sebum classifies biomarker classes for the diagnosis of Parkinson’s disease. *J. Am. Chem. Soc.* **2022**, *2*, 2013–2022. [[CrossRef](#)]
120. Fu, W.; Xu, L.; Yu, Q.; Fang, J.; Zhao, G.; Li, Y.; Pan, C.; Dong, H.; Wang, D.; Ren, H.; et al. Artificial intelligent olfactory system for the diagnosis of Parkinson’s disease. *ACS Omega* **2022**, *7*, 4001–4010. [[CrossRef](#)]
121. Trivedi, D.K.; Sinclair, E.; Xu, Y.; Sarkar, D.; Walton-Doyle, C.; Liscio, C.; Banks, P.; Milne, J.; Silverdale, M.; Kunath, T.; et al. Discovery of volatile biomarkers of Parkinson’s disease from sebum. *ACS Cent. Sci.* **2019**, *5*, 599–606. [[CrossRef](#)] [[PubMed](#)]
122. Sinclair, E.; Walton-Doyle, C.; Sarkar, D.; Hollywood, K.A.; Milne, J.; Lim, S.H.; Kunath, T.; Rijs, A.M.; de Bie, R.M.A.; Silverdale, M.; et al. Validating differential volatilome profiles in Parkinson’s disease. *ACS Cent. Sci.* **2021**, *7*, 300–306. [[CrossRef](#)] [[PubMed](#)]
123. Morgan, J. Joy of super smeller: Sebum clues for PD diagnostics. *Lancet Neurol.* **2016**, *15*, 138–139. [[CrossRef](#)] [[PubMed](#)]
124. Wang, R. Comparison of Decision Tree, Random Forest and Linear Discriminant Analysis Models in Breast Cancer Prediction. In *Proceedings of the Journal of Physics: Conference Series*; Institute of Physics: London, UK, 2022; Volume 2386.
125. Šimundić, A.-M. Measures of Diagnostic Accuracy: Basic Definitions. *EJIFCC* **2009**, *19*, 203–211. [[PubMed](#)]

126. Hajian-Tilaki, K. Receiver Operating Characteristic (ROC) Curve Analysis for Medical Diagnostic Test Evaluation. *Casp. J. Intern. Med.* **2013**, *4*, 627.
127. Wald, N.J.; Bestwick, J.P. Is the Area under an ROC Curve a Valid Measure of the Performance of a Screening or Diagnostic Test? *J. Med. Screen* **2014**, *21*, 51–56. [[CrossRef](#)]
128. Shang, G.; Dinh, D.; Mercer, T.; Yan, S.; Wang, S.; Malaei, B.; Luo, J.; Lu, S.; Zhong, C.-J. Chemiresistive sensor array with nanostructured interfaces for detection of human breaths with simulated lung cancer breath VOCs. *ACS Sens.* **2023**, *8*, 1328–1338. [[CrossRef](#)]
129. Bhattacharyya, N.; Mukherjee, D.; Singh, S.; Ghosh, R.; Karmakar, S.; Mallick, A.; Chattopadhyay, A.; Mondal, P.; Mondal, T.; Bhattacharyya, D.; et al. “Seeing” invisible volatile organic compound (VOC) marker of urinary bladder cancer: A development from bench to bedside prototype spectroscopic device. *Biosens. Bioelectron.* **2022**, *218*, 114764. [[CrossRef](#)]
130. Jian, Y.; Zhang, N.; Liu, T.; Zhu, Y.; Wang, D.; Dong, H.; Guo, L.; Qu, D.; Jiang, X.; Du, T.; et al. Artificially intelligent olfaction for fast and noninvasive diagnosis of bladder cancer from Urine. *ACS Sens.* **2022**, *7*, 1720–1731. [[CrossRef](#)]
131. Giró Benet, J.; Seo, M.; Khine, M.; Gumà Padró, J.; Pardo Martnez, A.; Kurdahi, F. Breast cancer detection by analyzing the volatile organic compound (VOC) signature in human urine. *Sci. Rep.* **2022**, *12*, 14873. [[CrossRef](#)]
132. Wang, P.Y.; Sun, Y.; Axel, R.; Abbott, L.F.; Yang, G.R. Evolving the olfactory system with machine Learning. *Neuron* **2021**, *109*, 3879–3892.e5. [[CrossRef](#)] [[PubMed](#)]
133. Sethi, S.; Nanda, R.; Chakraborty, T. Clinical Application of Volatile Organic Compound Analysis for Detecting Infectious Diseases. *Clin. Microbiol. Rev.* **2013**, *26*, 462–475. [[CrossRef](#)] [[PubMed](#)]
134. Belizário, J.E.; Faintuch, J.; Malpartida, M.G. Breath Biopsy and Discovery of Exclusive Volatile Organic Compounds for Diagnosis of Infectious Diseases. *Front. Cell. Infect. Microbiol.* **2021**, *10*, 564194. [[CrossRef](#)] [[PubMed](#)]
135. Ariga, K.; Nishikawa, M.; Mori, T.; Takeya, J.; Shrestha, L.K.; Jonathan, P.; Hill, J.P. Self-assembly as a key player for materials nanoarchitectonics. *Sci. Technol. Adv. Mater.* **2019**, *20*, 51–95. [[CrossRef](#)]
136. Harada, A.; Takashima, Y.; Hashidzume, A.; Yamaguchi, H. Supramolecular polymers and materials formed by host-guest interactions. *Bull. Chem. Soc. Jpn.* **2021**, *94*, 2381–2389. [[CrossRef](#)]
137. Ariga, K.; Jia, X.; Song, J.; Hill, J.P.; Leong, D.T.; Jia, Y.; Li, J. Nanoarchitectonics beyond self-assembly: Challenges to create bio-like hierarchic organization. *Angew. Chem. Int. Ed.* **2020**, *59*, 15424–15446. [[CrossRef](#)]
138. Kim, M.; Firestein, K.L.; Fernando, J.F.S.; Xu, X.; Lim, H.; Golberg, D.V.; Na, J.; Kim, J.; Tang, J.; Yamauchi, Y. Strategic design of Fe and N co-doped hierarchically porous carbon as superior ORR catalyst: From the perspective of nanoarchitectonics. *Chem. Sci.* **2022**, *13*, 10836–10845. [[CrossRef](#)]
139. Aono, M.; Ariga, K. The way to nanoarchitectonics and the way of nanoarchitectonics. *Adv. Mater.* **2016**, *28*, 989–992. [[CrossRef](#)]
140. Ariga, K. Nanoarchitectonics: A navigator from materials to life. *Mater. Chem. Front.* **2017**, *1*, 208–211. [[CrossRef](#)]

Disclaimer/Publisher’s Note: The statements, opinions and data contained in all publications are solely those of the individual author(s) and contributor(s) and not of MDPI and/or the editor(s). MDPI and/or the editor(s) disclaim responsibility for any injury to people or property resulting from any ideas, methods, instructions or products referred to in the content.